

Magnetoelectric effect and magnetic phase transitions in $(\text{Fe}_x\text{Cr}_{1-x})_2\text{O}_3$ single crystals

Yu. F. Popov, D. V. Belov, G. P. Vorob'ev, A. M. Kadomtseva, and M. M. Lukina

M. V. Lomonosov Moscow State University, 119899 Moscow, Russia

A. K. Zvezdin and M.-M. Tegeranchi

Institute of General Physics, Russian Academy of Sciences, 117942 Moscow, Russia

(Submitted 12 July 1995)

Zh. Éksp. Teor. Fiz. **109**, 891–901 (March 1996)

The magnetoelectric effect in $(\text{Fe}_x\text{Cr}_{1-x})_2\text{O}_3$ ($x=0,0.02,0.05,0.1$) single crystals has been studied under a magnetic field of up to 200 kOe. We have found that various magnetic phase transitions due to the restructuring of the spatial spin structure, and leading to radical changes in the magnetoelectric effect, take place in substitutional alloys. We have also detected a spontaneous phase transition from a conical spiral to a cycloidal spin structure at $x=0.1$ and a temperature of 45 K. The experimental data are in agreement with the theoretical thermodynamic model and can be accounted for in terms of competition among exchange energies of different modes. © 1996 American Institute of Physics. [S1063-7761(96)01403-6]

1. INTRODUCTION

The magnetoelectric effect is a sensitive tool for studying magnetic phase transitions induced by external fields. The magnetoelectric effect due to a strong magnetic field was first studied in Cr_2O_3 crystals, in which a linear magnetoelectric effect was predicted theoretically¹ and detected experimentally.² It was found that diagonal components of the linear magnetoelectric effect in Cr_2O_3 vanish at the field of the spin-flop transition.^{3–5} New nonlinear and non-reciprocal magneto-optical effects due to linear magnetoelectric interaction were also detected in Cr_2O_3 .^{6,7} Recent studies demonstrate that the linear magnetoelectric effect is very susceptible to the presence of a spatially modulated spin structure. Measurements⁸ of the electric polarization in BiFeO_3 in a strong magnetic field revealed jumps due to the disintegration of spatially modulated spin structure in a field of about 200 kOe. Cycloidal spin structure in BiFeO_3 at zero magnetic field was discovered via neutron diffraction.⁹ This structure results from Lifshitz relativistic exchange invariants, which are linear in derivatives of the order parameter in the D_{3d}^6 group.

In this work we have studied the magnetoelectric effect and phase transitions induced by a strong magnetic field in a set of fabricated rhombohedral $(\text{Fe}_x\text{Cr}_{1-x})_2\text{O}_3$ crystals. By recording field and temperature curves of the magnetoelectric effect in these crystals, we have detected features which can be interpreted in terms of phase transitions between different spatially modulated spin structures. Earlier,¹⁰ spin structure shaped as a conical helix was detected in this material using neutron diffraction. Magnetoelectric measurements of single crystals yield additional information about such structures and phase transitions between them. This work is a continuation of our previous study concerning the relationship between the magnetoelectric effect and spatially modulated spin structures in the bismuth ferrite BiFeO_3 .⁸ The magnetoelectric effect due to magnetic restructuring in $(\text{Fe}_x\text{Cr}_{1-x})_2\text{O}_3$ has been studied for the first time. These effects are of fundamental importance because in these mate-

rials the spatially modulated spin structure is defined not by relativistic interactions, but by different signs of indirect exchange in different pairs of interacting d -ions, which can affect phase transitions induced by an external field.

2. THERMODYNAMIC POTENTIAL AND PHASE DIAGRAM

The magnetic structure of Cr_2O_3 and $\alpha\text{-Fe}_2\text{O}_3$ can be described by the magnetic modes^{11,12}

$$\begin{aligned}L_A &= \mathbf{M}_1 - \mathbf{M}_2 + \mathbf{M}_3 - \mathbf{M}_4, \\L_B &= \mathbf{M}_1 - \mathbf{M}_2 - \mathbf{M}_3 + \mathbf{M}_4,\end{aligned}\quad (1)$$

respectively. Each of these modes is transformed according to an irreducible representation of the so-called exchange symmetry group.¹³ As the parameter x varies between 0 and 1, a phase transition between these two modes should take place ($x_{\text{cr}} \approx 0.2$).¹⁰ In a general case, the magnetic structure of the mixed compound $(\text{Fe}_x\text{Cr}_{1-x})_2\text{O}_3$ must be described by the combined order parameter $\eta = (L_A, L_B)$ corresponding to a reducible representation of the exchange symmetry group. But at $x < x_{\text{cr}}$ the L_A mode is sufficient. Hereinafter the index A of the vector L_A will be omitted. One feature of the $(\text{Fe}_x\text{Cr}_{1-x})_2\text{O}_3$ system is that it contains spatially modulated spin structure, but its symmetry (D_{3d}^6 group) excludes invariants from its thermodynamic potential that are linear in the spatial derivatives. In this case it is natural to consider an exchange mechanism that produces spatially modulated spin structures.

The thermodynamic potential of the $(\text{Fe}_x\text{Cr}_{1-x})_2\text{O}_3$ system with nonuniform exchange can be expressed as

$$\Phi = \frac{1}{V} \int \Phi(\theta, \nabla\theta, \nabla^2\theta) dr, \quad (2)$$

where the thermodynamic potential density is

$$\begin{aligned}\Phi &= K_1 \sin^2 \theta + K_2 \sin^4 \theta - \frac{\Delta\chi}{2} H^2 \\&\quad \times \sin^2 \theta + \gamma(\nabla L)^2 + \alpha(\nabla^2 L)^2.\end{aligned}\quad (3)$$

Here K_1 and K_2 are magnetic anisotropy constants, $\mathbf{L}=(\sin \theta \sin \varphi, \sin \theta \cos \varphi, \cos \theta)$ is the antiferromagnetism unit vector (θ and φ are the polar and azimuthal angles), $\Delta \chi$ is the difference between the transverse and longitudinal susceptibilities, $\Delta \chi=\chi_{\perp}-\chi_{\parallel}$, H is the external magnetic field, and α and γ are the nonuniform exchange constants. The thermodynamic potential in this form has been widely used to describe long-wave incommensurable structures resulting from exchange¹⁴ between our system and those described previously¹⁴ is that the order parameter in Eq. (3) is three-dimensional, and transforms according to a reducible representation, which is a direct product of the two- and one-dimensional irreducible representations of the \tilde{D}_{3d}^6 group.¹²⁻¹⁴ Therefore, transitions between incommensurable phases and between incommensurable and commensurable phases in this case are combined with spin alignment transitions. As a result, the phase diagram and the pattern of changes in physical parameters due to the transitions are more complicated. Microscopically, this specific nonuniform exchange ($\alpha>0$, $\gamma<0$) results from competing interactions in the system; in the present case we consider the competition between interactions generating the modes L_A and L_B .

We limit our consideration of incommensurable phases to the one-dimensional case, assuming that either θ or φ is constant.

2.1. Let us first consider the case $\theta=\text{const}$, $\varphi=\varphi(z)$. After substituting these equations into Eq. (3), we obtain the thermodynamic potential density in the form

$$\Phi=K_1 \sin^2 \theta+K_2 \sin^4 \theta-\frac{\Delta \chi}{2} H^2 \sin^2 \theta+\{\gamma(\varphi')^2+\alpha[(\varphi'')^2+(\varphi')^4]\} \sin^2 \theta. \quad (4)$$

The equation for extrema of the thermodynamic potential in Eq. (4), i.e.,

$$\frac{\partial \Phi}{\partial \eta}-\frac{d \partial \Phi}{d z\left(\frac{\partial \eta}{\partial z}\right)}+\frac{d^2 \partial \Phi}{d z^2 \partial\left(\frac{\partial^2 \eta}{\partial z^2}\right)}=0 \quad (5)$$

($\eta=\varphi$) takes the form

$$\alpha \frac{d^4 \varphi}{d z^4}-\gamma \frac{d^2 \varphi}{d z^2}-6 \alpha\left(\frac{d \varphi}{d z}\right)^2 \frac{d^2 \varphi}{d z^2}=0 \quad (6)$$

and, obviously, has a particular solution

$$\varphi=q z. \quad (7)$$

Substituting this solution into Eq. (4), we have

$$\Phi_1=\left(K_1-\frac{\Delta \chi}{2} H^2+\gamma q^2+\alpha q^4\right) \sin^2 \theta+K_2 \sin^4 \theta. \quad (8)$$

Minimizing the thermodynamic potential by varying q , we obtain

$$q^2=-\frac{\gamma}{2 \alpha}, \quad \gamma<0, \quad \alpha>0, \quad (9)$$

where q is the magnitude of the wave vector.

Substitution of Eq. (9) into Eq. (8) yields

$$\Phi_1=\left(K_1-\frac{\Delta \chi}{2} H^2-\frac{\gamma^2}{4 \alpha}\right) \sin^2 \theta+K_2 \sin^4 \theta. \quad (10)$$

Minimization of the thermodynamic potential in Eq. (10) with respect to θ yields the following equilibrium phases:

a) the uniform antiferromagnetic phase A in which

$$L \parallel c, \quad \theta=0 \text{ or } \pi, \quad \Phi_A=0. \quad (11)$$

b) the conical spiral C_1 with $0<\theta<\pi$ and

$$\Phi_{C_1}=-\frac{K_1-\frac{\Delta \chi}{2} H^2-\frac{\gamma^2}{4 \alpha}}{4 K_2}, \quad (12)$$

$$\sin^2 \theta=-\frac{K_1-\frac{\Delta \chi}{2} H^2-\frac{\gamma^2}{4 \alpha}}{4 K_2}, \quad \varphi=q z, \quad (12a)$$

where

$$\left|K_1-\frac{\Delta \chi}{2} H^2-\frac{\gamma^2}{4 \alpha}\right| \leq 4 K_2.$$

c) the conical spiral C_2 with $\theta=\pi/2$ and

$$\Phi_{C_2}=K_1-\frac{\Delta \chi}{2} H^2-\frac{\gamma^2}{4 \alpha}+K_2, \quad \varphi=q z. \quad (13)$$

2.2. In the case $\varphi=\text{const}$, $\theta=\theta(z)$, the thermodynamic potential density in Eq. (3) takes the form

$$\Phi_2=K_1 \sin^2 \theta+K_2 \sin^4 \theta-\frac{\Delta \chi}{2} H^2 \sin^2 \theta+\gamma(\theta')^2+\alpha[(\theta'')^2+(\theta')^4]. \quad (14)$$

Note that the last summand contains $(\theta')^4$ (see also Eq. (4)), which is often omitted in similar models.¹⁴ It emerges in our calculations because we express the order parameter in terms of the angular variables θ and φ , and this summand is of primary importance.

Equation (5) for extrema of the thermodynamic potential in Eq. (14) at $\eta=0$ takes the form

$$\sin^2 \theta\left[K_1-\frac{\Delta \chi}{2} H^2+2 K_2 \sin^2 \theta\right]+\frac{d^2 \theta}{d z^2}\left[6 \alpha\left(\frac{d \theta}{d z}\right)^2+\gamma\right]-\alpha \frac{d^4 \theta}{d z^4}=0. \quad (15)$$

In general, no analytic solution of this equation is known, but if the anisotropy energy is much lower than the exchange energy, it has the approximate particular solution

$$\theta=q z, \quad (16)$$

where q is also defined by Eq. (9). This approximate solution corresponds to the sine-wave or one-harmonic approximation, which is often used in the theory of spatially modulated spin structures.¹⁴

The function in Eq. (16) describes the cycloidal phase C_y , whose thermodynamic potential defined by Eq. (14) is converted with due account of Eqs. (15) and (9) to

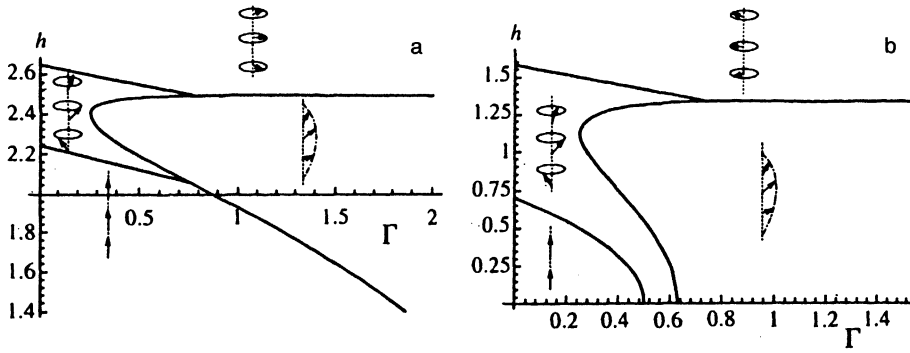


FIG. 1. Theoretical phase diagram in h - Γ coordinates, where $h = \sqrt{\Delta\chi/2K_2}H$ is the dimensionless magnetic field, $\Gamma = \gamma^2/4\alpha K_2$ calculated at (a) $k=K_1/K_2=5$ and (b) 0.5.

$$\Phi_{cr} = \frac{1}{2} \left(K_1 - \frac{\Delta\chi}{2} H^2 \right) + \frac{3}{8} K_2 - \frac{\gamma^2}{4\alpha}, \quad (17)$$

which takes into account that

$$\frac{1}{V} \int dr \sin^2 \theta = \frac{1}{2}, \quad \frac{1}{V} \int dr \sin^4 \theta = \frac{3}{8}.$$

In the $(\text{Fe}_x\text{Cr}_{1-x})_2\text{O}_3$ system studied here, various phase transitions among phases A , C_1 , C_2 , and C_y are possible as the parameters x , H , and T vary. Figure 1 shows a phase diagram of this system plotted in dimensionless coordinates

$$k = \frac{K_1}{K_2}, \quad h^2 = \frac{\Delta\chi}{2K_2} H^2, \quad \Gamma = \frac{\gamma^2}{4\alpha K_2}, \quad E = \frac{\Phi}{K_2}.$$

The diagram in Fig. 1a was calculated at $k=5$, and that in Fig. 1b at $k=0.5$.

Phase transitions between the cycloidal phase C_y and the phases A , C_1 , and C_2 are first order, and equations of phase transition curves can be derived from the equality of potentials in respective phases:

$$\begin{aligned} C_y - A: \quad E_{cr} &= E_A, \quad h_C^2 = k + \frac{3}{4} - 2\Gamma, \\ C_y - C_2: \quad E_{cr} &= E_{C_2}, \quad h_C^2 = k + \frac{5}{4}, \\ C_y - C_1: \quad E_{cr} &= E_{C_1}, \quad h_C^2 = k + 1 - \Gamma \pm \left(2\Gamma - \frac{1}{2} \right)^{1/2}. \end{aligned} \quad (18)$$

The equations for second-order transition curves are derived from the condition $\Phi''=0$:

$$\begin{aligned} A - C_1: \quad h_C^2 &= k - \Gamma, \\ C_1 - C_2: \quad h_C^2 &= k + 2 - \Gamma. \end{aligned} \quad (19)$$

The phase diagram in Fig. 1 can be transformed to an H - T diagram, given the parameters K_1 , K_2 , α , and γ as functions of temperature, which are as yet unknown. The importance of the h - Γ diagram in Fig. 1 derives from the fact that it yields a representation of the topology of the H - T phase diagram, and shows the sequence of feasible phase transitions due to a magnetic field.

3. LINEAR MAGNETOELECTRIC EFFECT

Various phase transitions induced by a magnetic field can be detected through the magnetoelectric effect. The electric polarization of $(\text{Fe}_x\text{Cr}_{1-x})_2\text{O}_3$ at small x , i.e., in a phase described by the magnetic mode L_A , can be expressed as⁸

$$\begin{aligned} P &= \chi_{\perp} (H - (HL)L) \\ &\times \begin{vmatrix} \lambda_1 L_y + \lambda_3 L_z & \lambda_1 L_x & \lambda_2 L_x \\ \lambda_1 L_x & -\lambda_1 L_y + \lambda_3 L_z & \lambda_2 L_y \\ \lambda_4 L_x & \lambda_4 L_y & \lambda_5 L_z \end{vmatrix} \\ &+ \chi_{\parallel} (HL) \begin{vmatrix} 2\lambda_1 L_x L_z + (\lambda_3 + \lambda_4) L_x L_y \\ \lambda_1 (L_x^2 - L_y^2) + (\lambda_3 + \lambda_4) L_y L_z \\ \lambda_2 (L_x^2 + L_y^2) + \lambda_5 L_z^2 \end{vmatrix}. \end{aligned} \quad (20)$$

In particular, the polarization component P_z measured in our work at $\mathbf{H}=(0,0,H)$ can be derived from Eq. (20):

$$P_z = \chi_{\perp} \lambda_5 L_z H - \lambda_2 \Delta\chi H L_z L_x^2 - \lambda_5 \Delta\chi H L_z^3, \quad (21)$$

where $L_x^2 = L_x^2 + L_y^2$. To be more exact, the term $\lambda_6 \chi_{\perp} L_y \times (L_y^2 - 3L_x^2)$ should be added to this formula in order to comply with the magnetic symmetry condition, but this term is negligible compared to those in Eq. (20) (of the second order in relativistic interactions) and is not detected in experiments, so it has been omitted. In spatially modulated phases the average polarization aligned with the c -axis,

$$\langle P_z \rangle = \frac{1}{V} \int dr P_z,$$

can be expressed as

$$\begin{aligned} \text{phase } A: \quad \langle P_z \rangle &= \alpha_{33} H_z, \\ \text{phase } C_y: \quad \langle P_z \rangle &= 0, \\ \text{phase } C_1: \quad \langle P_z \rangle &= \alpha_{33} \cos \theta H_z (1 - \delta \sin^2 \theta), \\ \text{phase } C_2: \quad \langle P_z \rangle &= 0, \end{aligned} \quad (22)$$

where $\theta(H)$ is defined by Eq. (12a), $\alpha_{33} = \chi_{\parallel} \lambda_5$, and $\delta = \Delta\chi(\lambda_2 - \lambda_3)/\chi_{\parallel} \lambda_5$.

Hence the magnitude of the magnetoelectric effect is radically changed by phase transitions due to an external magnetic field. For example, curves of the electric polarization plotted against magnetic field affected by the phase transitions $A - C_1 - C_2$, $A - C_1 - C_y - C_1 - C_2$, $C_y - C_1 - C_2$ may have shapes calculated at various parameters k , Γ , and

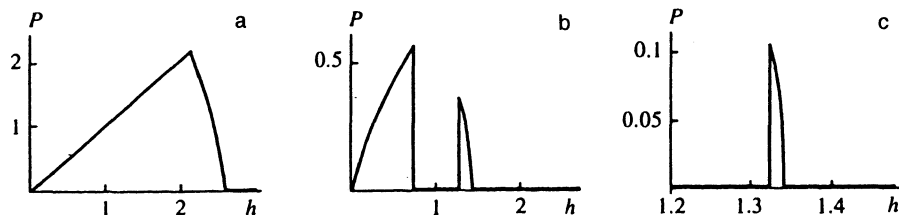


FIG. 2. Calculated curves of the electric polarization versus magnetic field illustrating the sequences of magnetic phase transitions: a) $A-C_1-C_2$ (at $k=5$, $\Gamma=0.2$, and $\delta=0.5$); b) $A-C_1-C_y-C_1-C_2$ (at $k=0.5$, $\Gamma=0.4$, and $\delta=0.5$); c) $C_y-C_1-C_2$ (at $k=0.5$, $\Gamma=0.7$, and $\delta=0.5$).

δ and shown in Fig. 2. Similar phase transitions in $(\text{Fe}_x\text{Cr}_{1-x})_2\text{O}_3$ may be caused by changes in the concentration of Fe^{3+} ions and temperature.

4. SAMPLES AND EXPERIMENTAL TECHNIQUES

We studied magnetic and magnetoelectric properties of rhombohedral $(\text{Fe}_x\text{Cr}_{1-x})_2\text{O}_3$ single crystals ($x=0, 0.02, 0.05, 0.1$). The crystals were $3 \times 4 \text{ mm}^2$ wafers $0.1-0.2 \text{ mm}$ thick, with the $[111]$ axis normal to their planes. The crystals were grown in an uncontrolled manner from a molten solution. The solvent was a mixture of potassium tetraborate and lead oxide in various proportions (depending on the desired composition). The crystals were synthesized by evaporating the mixture at a constant temperature of $1210-1230 \text{ }^\circ\text{C}$. The chemical composition was determined to within 3% using X-ray spectroscopy.

In order to detect magnetic restructuring in a field, we measured the magnetoelectric effect, i.e., the electric polarization P induced by a pulsed magnetic field of up to 200 kOe in the temperature range 4.2 to 300 K. The i th electric polarization component in a plane perpendicular to the i axis was measured using epoxy electrodes with a conducting filler connected to a high-impedance electrometer stage and an oscilloscope. The oscilloscope detected the voltage across the electrodes, $U_i \approx P_i$, as a function of magnetic field H .⁸ Since the input capacitance of the stage was compensated for, the device sensitivity was high, and it could detect a surface charge density down to 10^{-7} C/m^2 . Since the crystals studied were wafers, we measured longitudinal components of the magnetoelectric effect.

Magnetic moments of single crystals were measured by a magnetic torsion balance with self-compensation under a dc magnetic field of up to 12 kOe.

5. MEASUREMENTS AND DISCUSSION

We have found that the crystals studied are antiferromagnetics with Néel temperatures of 309, 302, 288, and 259 K at $x=0, 0.02, 0.05$, and 0.1 , respectively. Note that the Néel temperature drops with the concentration of Fe^{3+} ions over the concentration range studied, probably due to the different signs and amplitudes of exchange interaction between different ions. In single crystals with the lowest Fe^{3+} content ($x=0.02$), as in Cr_2O_3 , a linear magnetoelectric effect was observed, and the magnetic susceptibility changed sign at a temperature of about 110 K and was considerably smaller than in Cr_2O_3 beyond this temperature. Under a sufficiently strong magnetic field H_c aligned with

the c -axis the magnetoelectric effect was zero, but the drop in electric polarization at H_c was less sharp than that due to the spin-flop transition in Cr_2O_3 (Fig. 3).

At $x=0.05$ the function $P_i(H_i)$ had a more complex shape in the temperature range 10–62 K. At $T=15 \text{ K}$, for example (Fig. 4), the magnetoelectric effect was detected only at $H > H_c = 80 \text{ K}$, where, according to Eqs. (18) and (22), phase transitions from a cycloidal spin structure C_y to a conical spiral C_1 can be induced by the magnetic field. At 29 K the magnetoelectric effect was small and essentially linear in the field at $H < H_c$, which is typical of this system, according to Eq. (22), if it is either a uniform antiferromagnetic or has the conical spiral spin structure C_1 . At a higher field ranging from 60 to 105 kOe the magnetoelectric effect is zero, which may result from a phase transition to the cycloidal spin structure C_y in this field range. At a field above 105 kOe the electric polarization reemerged and disappeared again, which may be due to a transition from the cycloidal structure to the conical spiral (C_y-C_1 transition) and the subsequent C_1-C_2 transition. According to the phase diagram in Figs. 1 and 2, this sequence of phase transitions, $A-C-1-C_y-C_1-C_2$, is quite feasible. A similar peculiar field dependence of the electric polarization was also observed at other temperatures (for example, 139 K and 150 K, Fig. 4). But the anomaly in the $P_i(H_i)$ curve due to $C_y-C_1-C_2$ transitions was small, and these transitions could not be detected at all temperatures (for example, 77 K and 182 K in Fig. 4). The magnetoelectric susceptibility at $x=0.05$ is a complex function of temperature and changes sign several times (Fig. 5), unlike that of Cr_2O_3 and at $x=0.02$, which changes sign only once.

The forward and backward $P_i(H_i)$ curves are usually

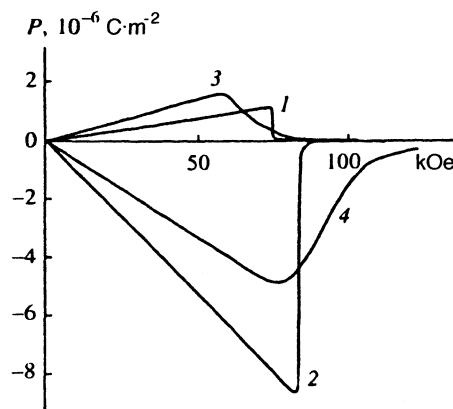


FIG. 3. Measured longitudinal electric polarization $P_z(H_z)$ versus magnetic field in Cr_2O_3 at (1) 77 K and (2) 150 K and in the alloy with $x=0.02$ at temperature of (3) 77 K and (4) 160 K.

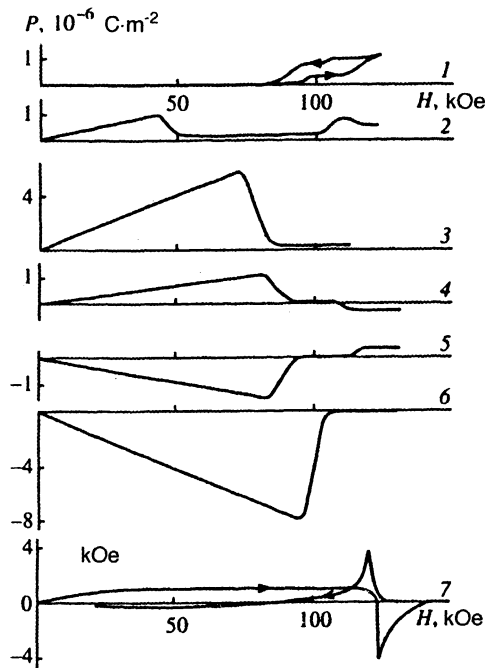


FIG. 4. Longitudinal electric polarization versus magnetic field in alloys with $x=0.05$ at (1) 15 K (2) 29 K, (3) 77 K, (4) 139 K, (5) 150 K, (6) 182 K, and (7) 266 K.

different, the hysteresis being larger at low temperatures and around the Néel temperature.

At $x=0.1$ the magnetoelectric effect was zero at a temperature of up to 45 K even in a strong magnetic field of up to 120 kOe, which may be due to cycloidal spin structure C_y (Fig. 5) in this temperature range. At a higher temperature a small electric polarization was detected in a magnetic field with a small cusp in the $P_i(H_i)$ curve, probably due to the conical spiral structure C_1 in a strong magnetic field (curve 1 in Fig. 6). At higher temperatures the electric polarization (magnetoelectric susceptibility) was a stronger function of the field, and breaks at phase transitions related to magnetic restructuring at H_c , yielding a vanishing magnetoelectric effect, were more pronounced (curves 2 and 3 in Fig. 6). The $H-T$ diagrams of the phase transition between the conical spiral C_1 and cycloidal structure C_y at $x=0.05$ and

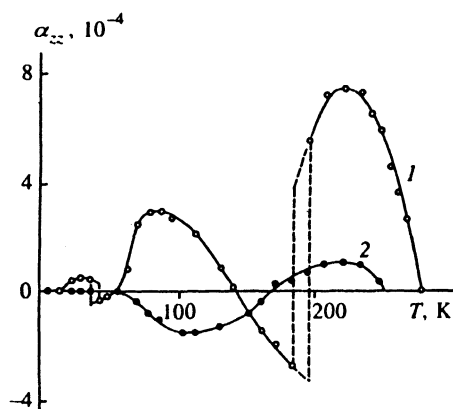


FIG. 5. Magneto-electric susceptibility versus temperature in alloys with (1) $x=0.05$ and (2) 0.1.

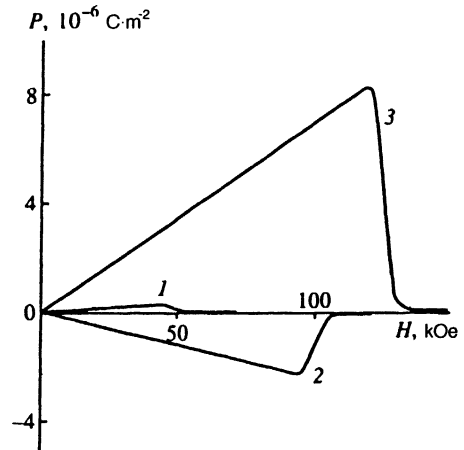


FIG. 6. Longitudinal electric polarization versus magnetic field in an alloy with $x=0.1$ at (1) 77 K, (2) 93 K, and (3) 194 K.

0.1 are given in Fig. 7. One can see that at low temperatures around 45 K at $x=0.1$ the threshold field changes rapidly and tends to zero at $T \approx 45$ K. Given that the magnetoelectric effect is zero below 45 K, it is natural to assume that a spontaneous phase transition from the conical spiral to the cycloidal structure, C_1-C_y , takes place in this material around 45 K. A similar spontaneous transition at 15 K is feasible at $x=0.05$. We could not detect the phase transition from the cycloidal C_y to spiral C_2 structure ($\theta = \pi/2$) since, according to Eq. (22), it should not lead to a change in the magnetoelectric effect.

6. CONCLUSION

We have detected new features in the field and temperature dependence of the magnetoelectric effect in $(\text{Fe}_x\text{Cr}_{1-x})_2\text{O}_3$ and interpreted them in terms of field-induced phase transitions either between the uniform antiferromagnetic phase and spatially modulated spin structures or between various spatially modulated structures. These phase transitions due to competing exchange interactions among various ions are controlled by the magnetic field, temperature, and iron content. We assume that the competition among different magnetic ordering modes leads to a strong effect of the iron content on the field and temperature dependences of the magnetoelectric effect in Cr_2O_3 , which is a highly sensitive indicator of restructuring in the magnetic ordering. For example, in the alloy with $x=0.05$ a set of transitions $A-C_1-C_y-C_1-C_2$ caused by the magnetic re-

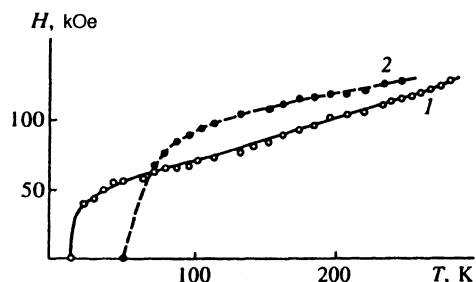


FIG. 7. Measured transition field in alloys with (1) $x=0.05$ and (2) 0.1.

structuring is observed. We have discovered a spontaneous $C_y - C_1$ transition at 45 K in the alloy with $x=0.1$.

The work was supported by the Russian Foundation for Fundamental Research (Grant No. 93-02-3214) and INTAS (Grant No. 94-935).

¹I. E. Dzyaloshinskii, Zh. Éksp. Teor. Fiz. **37**, 881 (1959).

²D. N. Astrov, Zh. Éksp. Teor. Fiz. **38**, 984 (1960) [Sov. Phys. JETP **11**, 708 (1960)].

³S. Foner and M. Hanabusa, J. Appl. Phys. **34**, 1246 (1963).

⁴J. Ohtani and K. Kohn, J. Phys. Soc. Jap. **53**, 3744 (1984).

⁵Yu. F. Popov, A. M. Kadomtseva, and Z. A. Kazei, JETP Lett. **55**, 234 (1992).

⁶B. B. Krichevskii, V. V. Pavlov, and R. V. Pisarev, Zh. Éksp. Teor. Fiz. **94**, 284 (1988).

⁷B. B. Krichevskii, V. V. Pavlov, R. V. Pisarev, and V. N. Gridnev, J. Phys. C: Condensed Matter **5**, 8233 (1993).

⁸Yu. F. Popov, A. K. Zvezdin, G. P. Vorob'ev *et al.*, JETP Lett. **57**, 69 (1993).

⁹I. Sosnowska, T. Peterlin-Neumaier, and E. Struchle, J. Phys. C **15**, 4835 (1982).

¹⁰D. Cox, W. Takei, and G. Shirane, J. Phys. Chem. Sol. **24**, 405 (1963).

¹¹Yu. A. Izyumov and R. P. Ozerov, *Magnetic Neutron Diffractometry* [in Russian], Nauka, Moscow (1966), p. 341.

¹²A. S. Borovik-Romanov, *Antiferromagnetism, Topics in Science* [in Russian], Akad. Nauk SSSR, Moscow (1962), p. 45.

¹³J.-C. Toledano and P. Toledano, *Landau Theory of Phase Transitions* [Russian translation], Mir, Moscow (1994), p. 103.

¹⁴Yu. A. Izyumov, *Neutron Diffraction by Long-Wave Periodic Structures* [in Russian], Énergoatomizdat, Moscow (1987), p. 65.

Translation was provided by the Russian Editorial office.